Supporting Information

Surface Plasmon-Photosensitizer Resonance Coupling: An Enhanced Singlet Oxygen Production Platform for Broad-Spectrum Photodynamic Inactivation of Bacteria

Bo Hu,[†] Xian Cao,[†] Keaton Nahan,[†] Joseph Caruso,[†] Hong Tang,[‡*] Peng Zhang[†]*

[†]Department of Chemistry, University of Cincinnati, Cincinnati, OH 45221, United States

[‡]Drug Discovery Center, University of Cincinnati, Cincinnati, OH 45237, United States

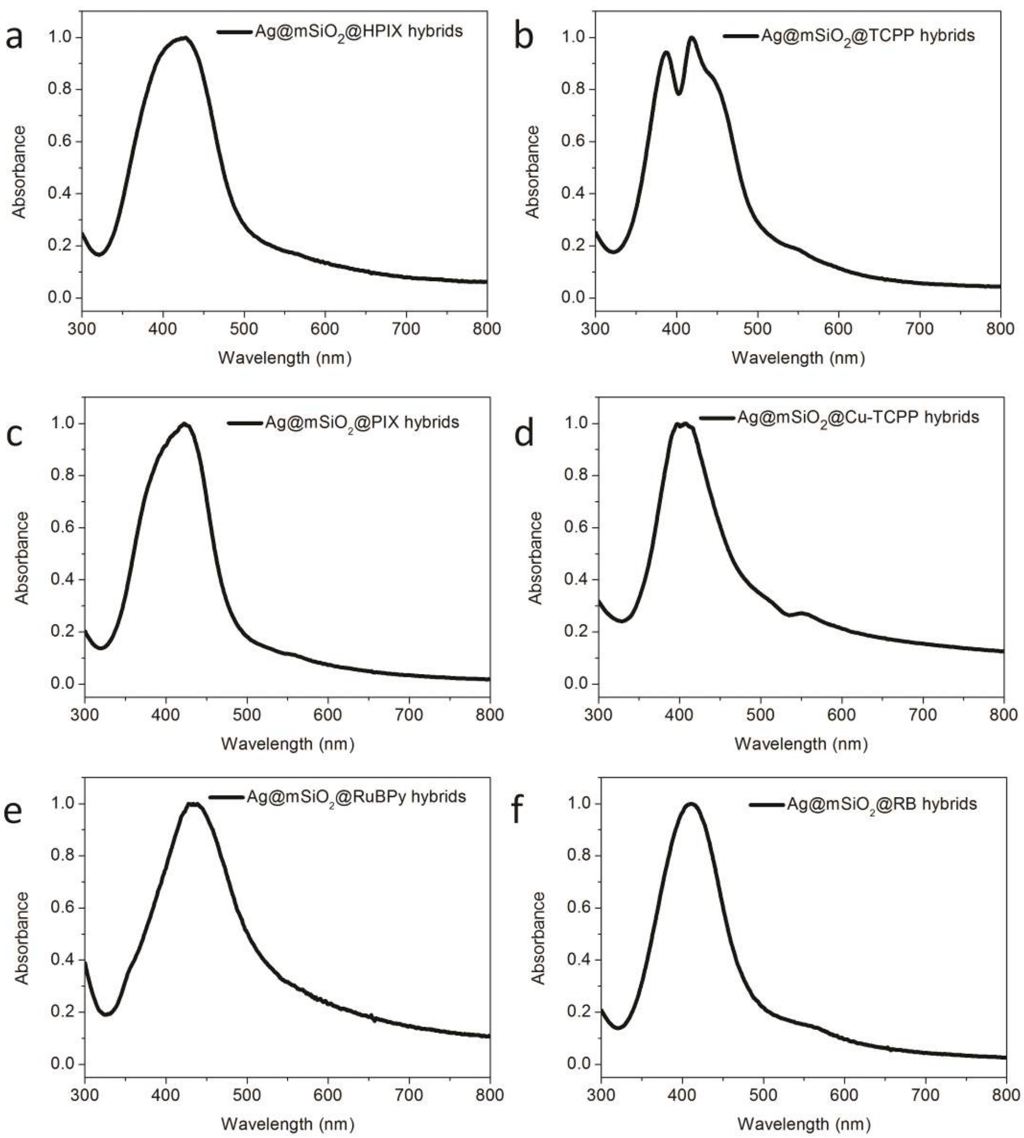

Fig. S1 UV-Vis absorption spectra of Ag@mSiO$_2$@photosensitizer hybrids, including HPIX (a), TCPP (b), PIX (c), Cu-TCPP (d), RuBPy (e), and RB (f).

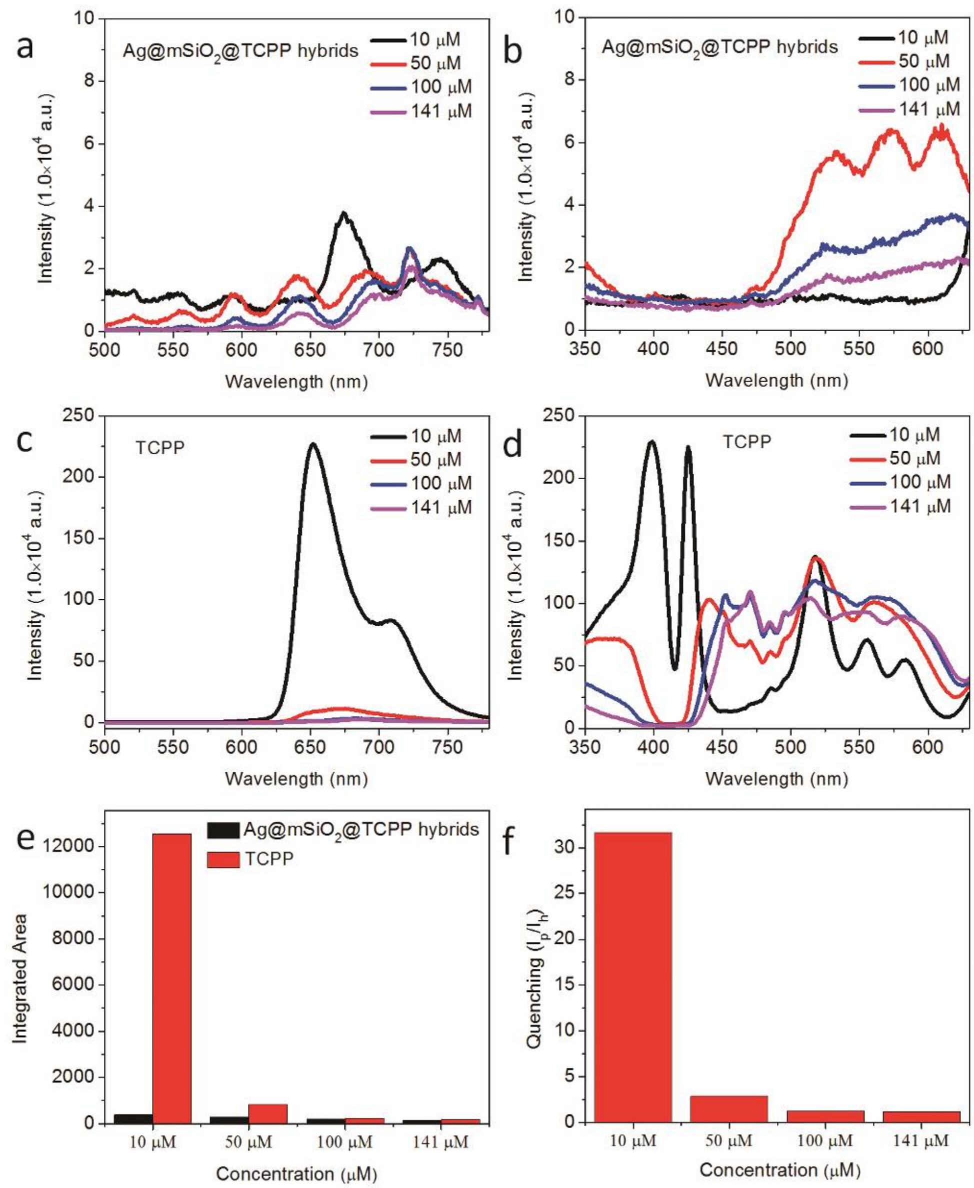

Fig. S2 Photoluminescence spectra of Ag@mSiO_2@TCPP hybrid and TCPP of different photosensitizer concentrations (10-141 μM). Emission spectra (a) and (c) are excited at 400 nm. Excitation spectra (b) and (d) are emitted at 650 nm for 10 μM, 672 nm for 50 μM, 682 nm for 100 μM, and 685 nm for 141 μM. (e) Relationship between integrated fluorescence signal (500-780 nm) and concentration of photosensitizer. (f) Relationship between fluorescence quenching of photosensitizer in hybrid (I_p/I_h) and concentration of photosensitizer.

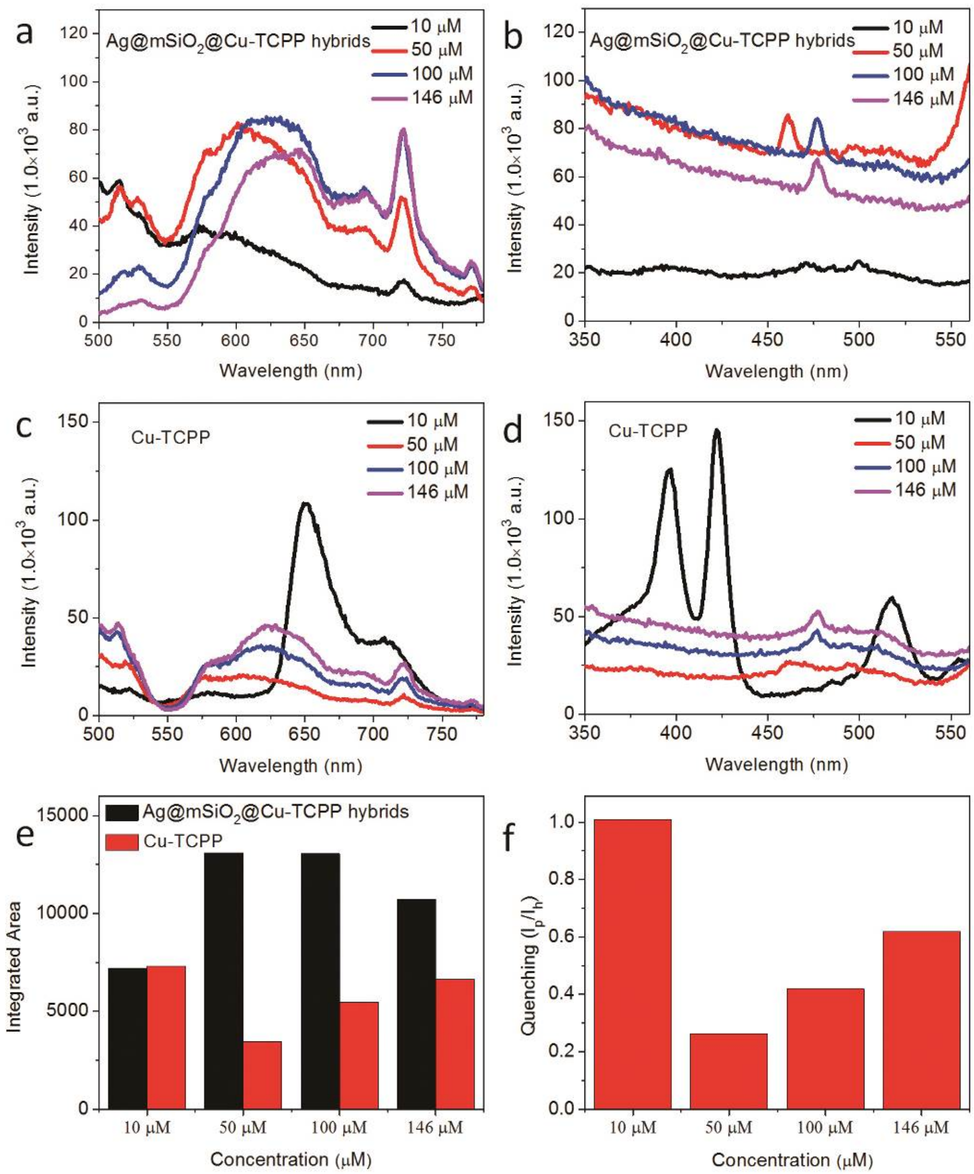

Fig. S3 Photoluminescence spectra of Ag@mSiO_2@Cu-TCPP hybrids and Cu-TCPP in different photosensitizer concentrations (10-146 μM). Emission spectra (a) and (c) are excited at 400 nm. Excitation spectra (b) and (d) are emitted at 650 nm for 10 μM, 600 nm for 50 μM, 620 nm for 100 μM, and 620 nm for 146 μM. (e) Relationship between integrated fluorescence signal (500-780 nm) and concentration of photosensitizer. (f) Relationship between fluorescence quenching of photosensitizer in hybrid (I_p/I_h) and concentration of photosensitizer.

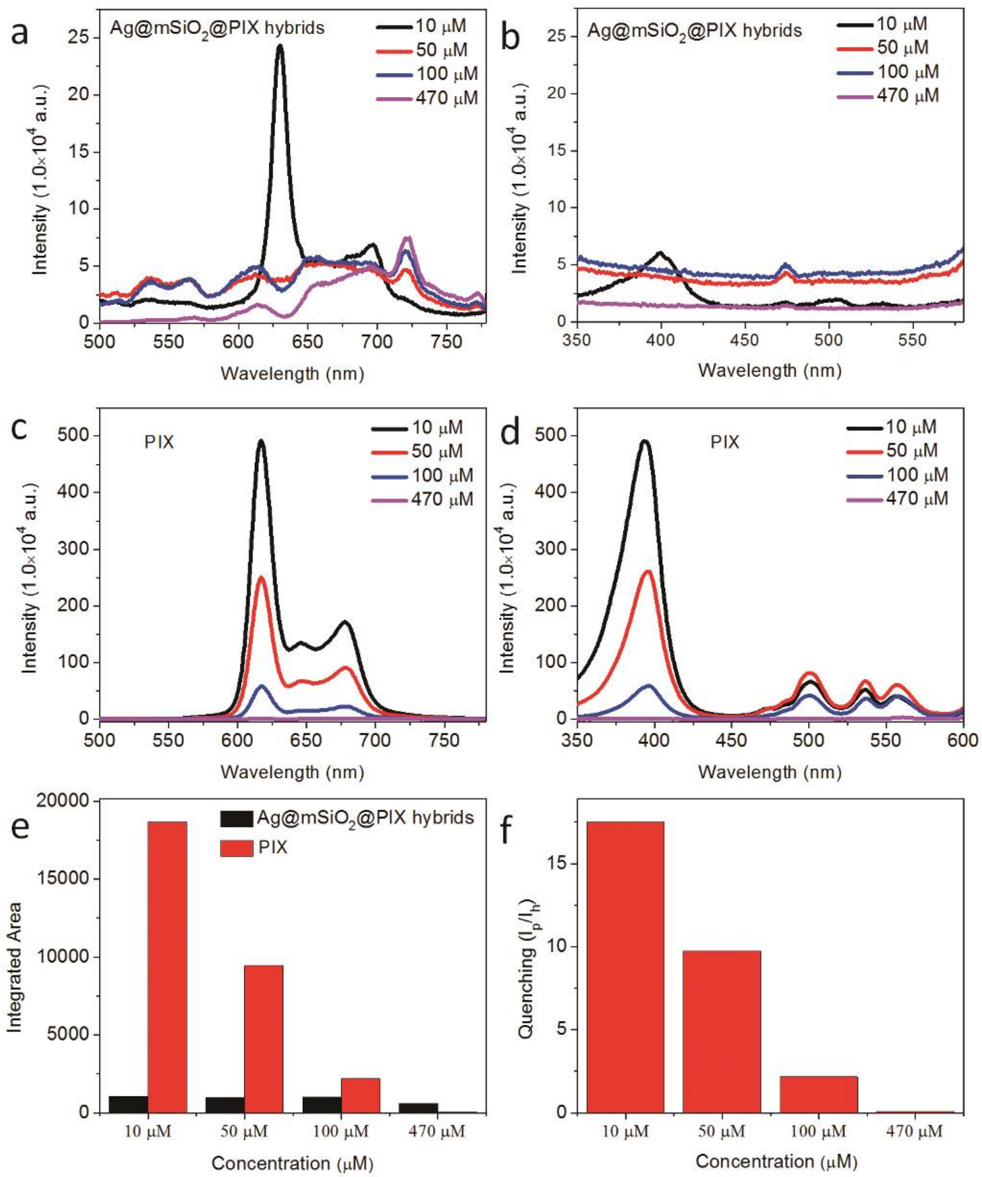

Fig. S4 Photoluminescence spectra of the Ag@mSiO$_2$@PIX hybrids and PIX in different photosensitizer concentrations (10-470 μM). Emission spectra (a) and (c) are excited at 393 nm. Excitation spectra (b) and (d) are emitted at 617 nm. (e) Relationship between integrated fluorescence signal (500-780 nm) and concentration of photosensitizer. (f) Relationship between fluorescence quenching of photosensitizer in hybrid (I_p/I_h) and concentration of photosensitizer.

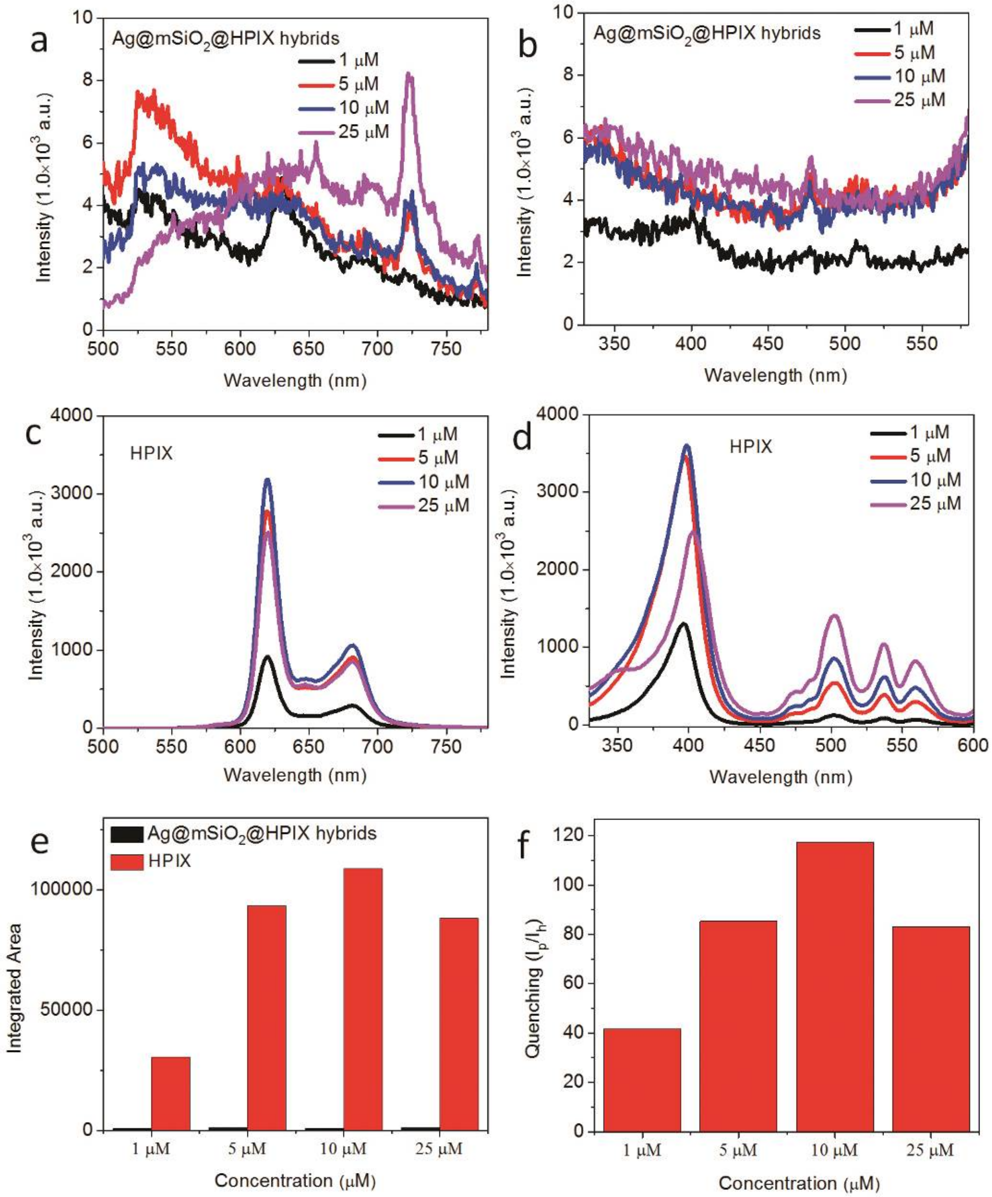

Fig. S5 Photoluminescence spectra of the Ag@mSiO_2@HPIX hybrids and HPIX in different photosensitizer concentrations (1-25 μM). Emission spectra (a) and (c) are excited at 403 nm. Excitation spectra (b) and (d) are emitted at 620 nm. (e) Relationship between integrated fluorescence signal (500-780 nm) and concentration of photosensitizer. (f) Relationship between fluorescence quenching of photosensitizer in hybrid (I_p/I_h) and concentration of photosensitizer.

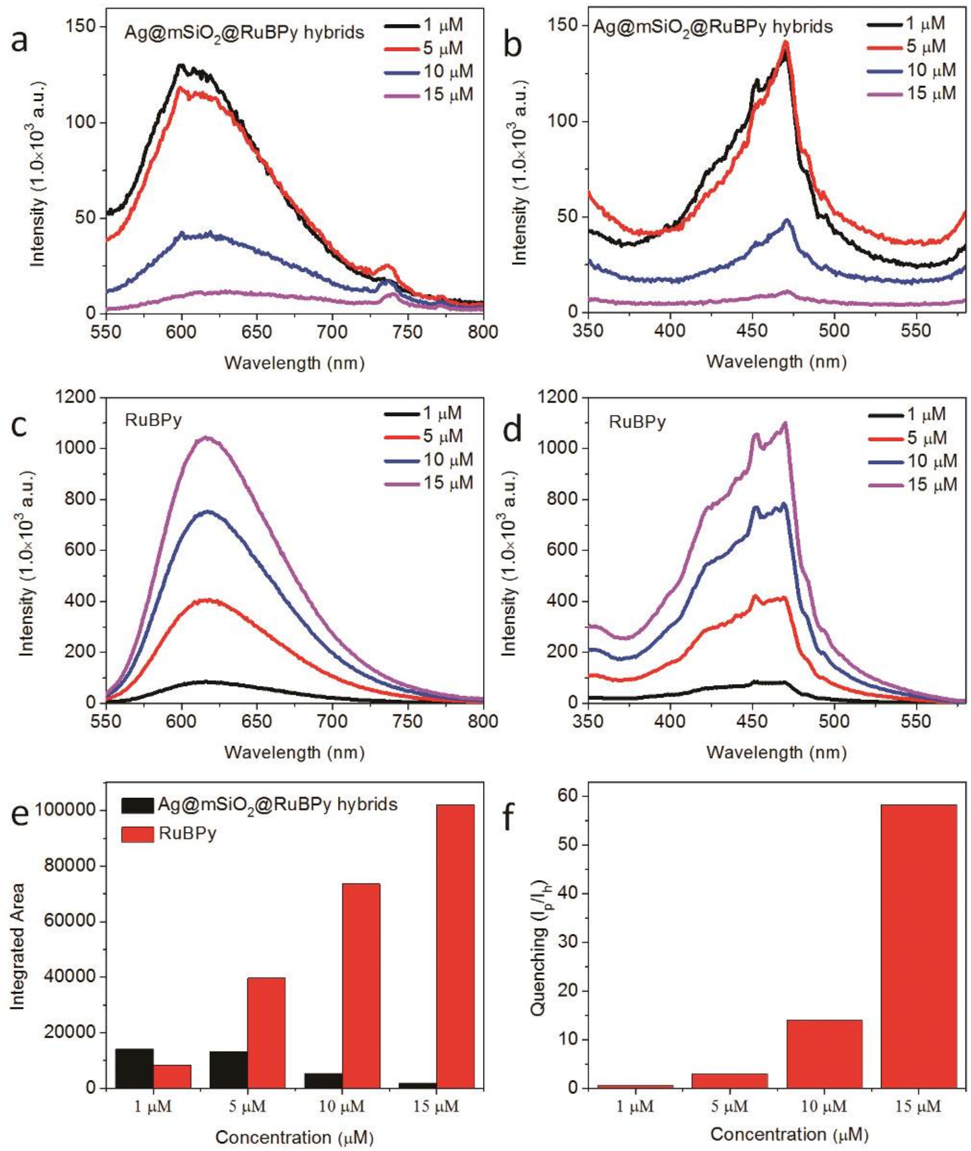

Fig. S6 Photoluminescence spectra of the Ag@mSiO_2@RuBPy hybrids and RuBPy in different photosensitizer concentrations (1-15 μM). Emission spectra (a) and (c) are excited at 460 nm. Excitation spectra (b) and (d) are emitted at 615 nm. (e) Relationship between integrated fluorescence signal (550-780 nm) and concentration of photosensitizer. (f) Relationship between fluorescence quenching of photosensitizer in hybrid (I_p/I_h) and concentration of photosensitizer.

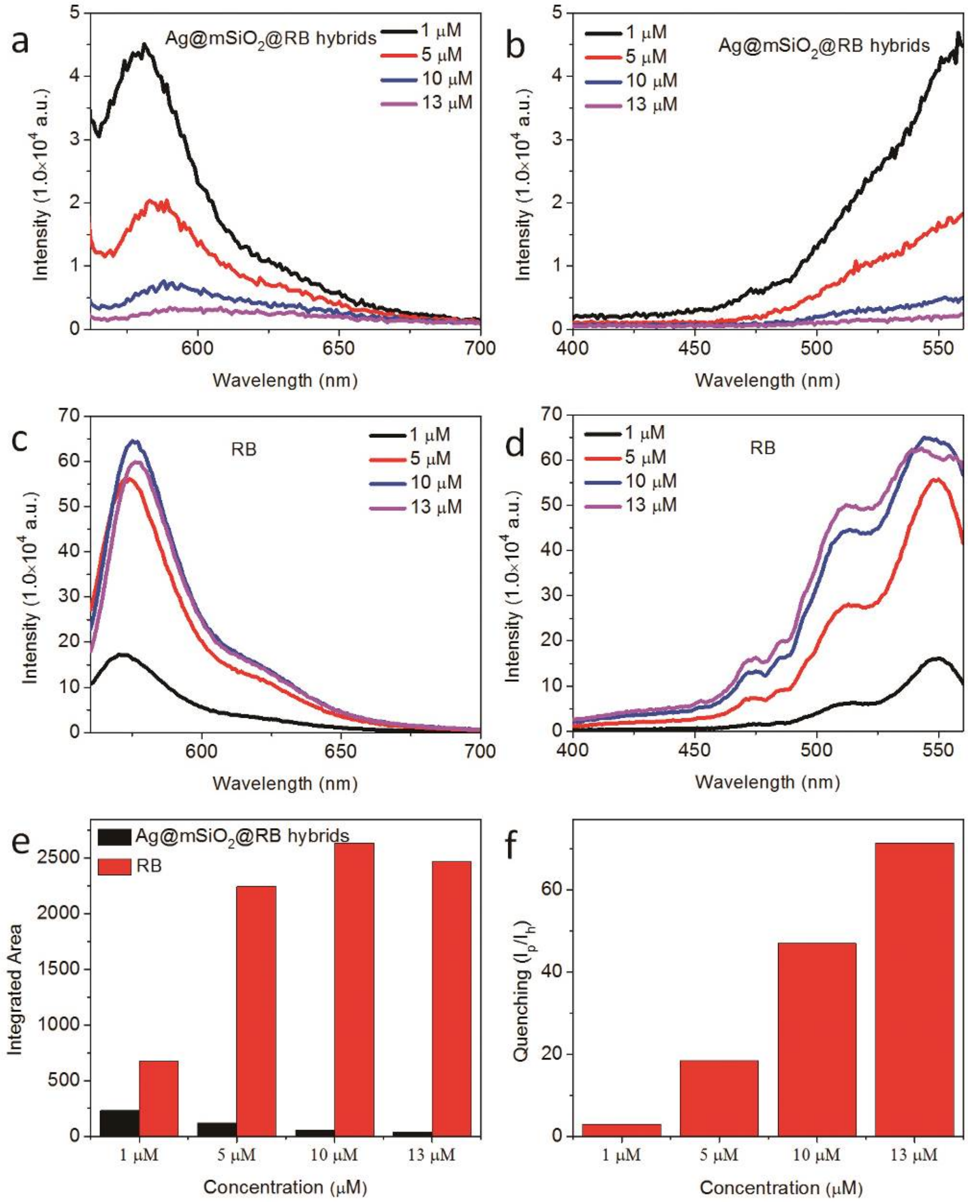

Fig. S7 Photoluminescence spectra of the Ag@mSiO_2@RB hybrids and RB in different photosensitizer concentrations (1-13 μM). Emission spectra (a) and (c) are excited at 550 nm. Excitation spectra (b) and (d) are emitted at 576 nm. (e) Relationship between integrated fluorescence signal (560-700 nm) and concentration of photosensitizer. (f) Relationship between fluorescence quenching of photosensitizer in hybrid (I_p/I_h) and concentration of photosensitizer.

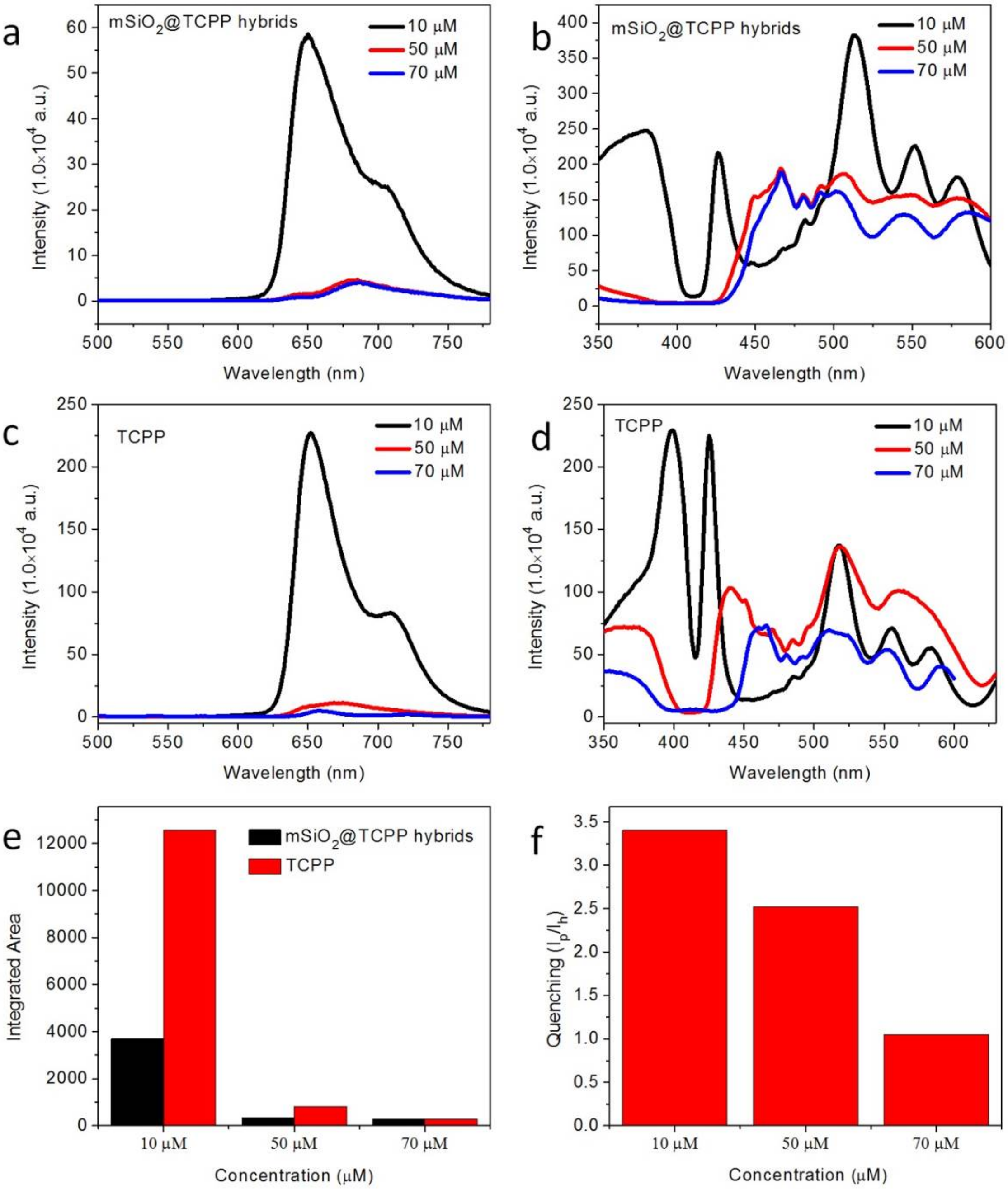

Fig. S8 Photoluminescence spectra of Ag@mSiO$_2$@TCPP hybrid after NaCN treatment and pure TCPP of different photosensitizer concentrations. Emission spectra (a) and (c) are excited at 400 nm. Excitation spectra (b) and (d) are emitted at 650 nm for 10 μM, 672 nm for 50 μM, and 685 nm for 70 μM. (e) Relationship between integrated fluorescence signal (500-780 nm) and TCPP concentration. (f) Relationship between fluorescence quenching of TCPP in hybrid (I_p/I_h) and TCPP concentration.

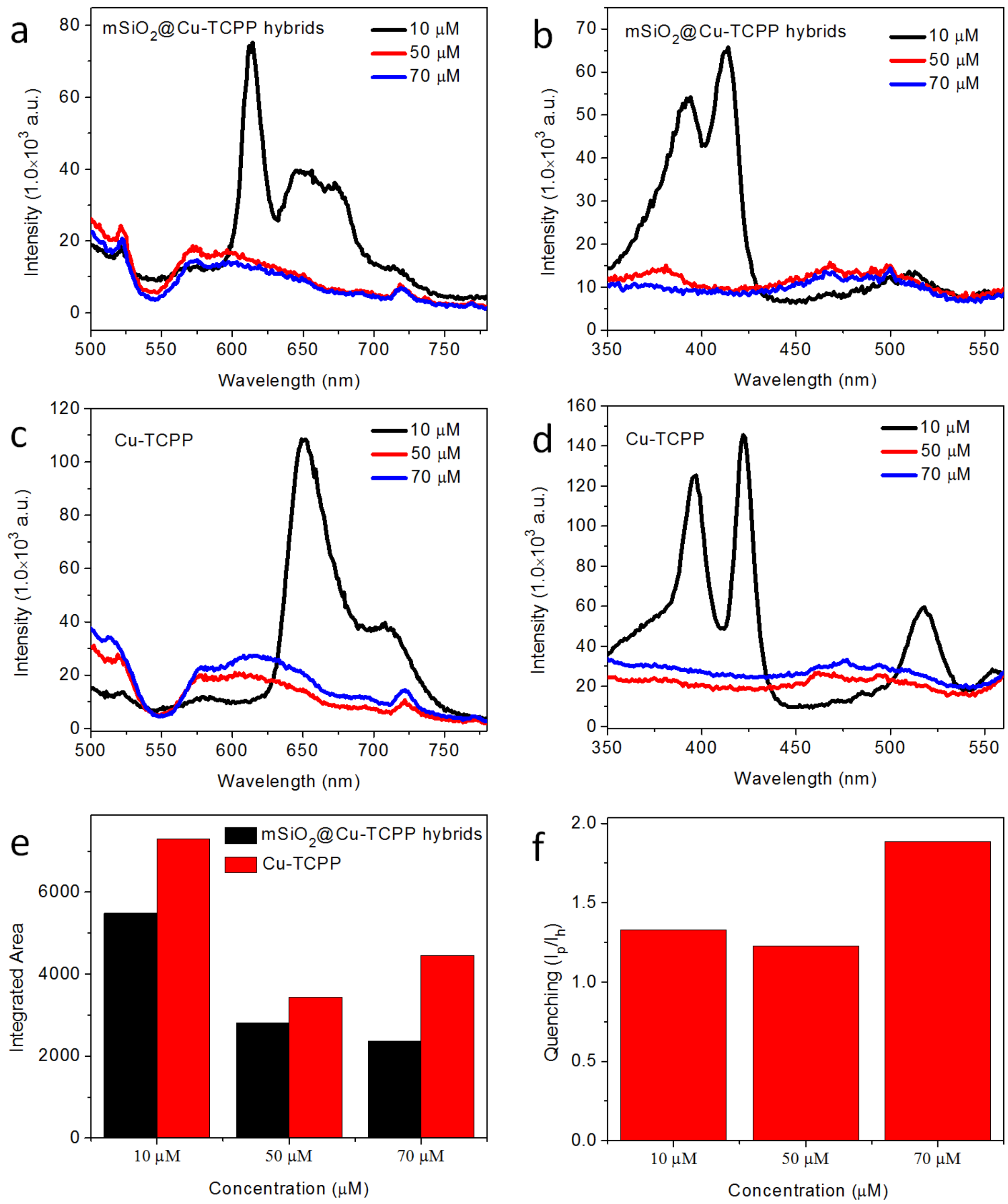

Fig. S9 Photoluminescence spectra of Ag@mSiO$_2$@Cu-TCPP hybrid after NaCN treatment and pure Cu-TCPP of different photosensitizer concentrations. Emission spectra (a) and (c) are excited at 400 nm. Excitation spectra (b) and (d) are emitted at 650 nm. (e) Relationship between integrated fluorescence signal (500-780 nm) and Cu-TCPP concentration. (f) Relationship between fluorescence quenching of Cu-TCPP in hybrid (I_p/I_h) and Cu-TCPP concentration.

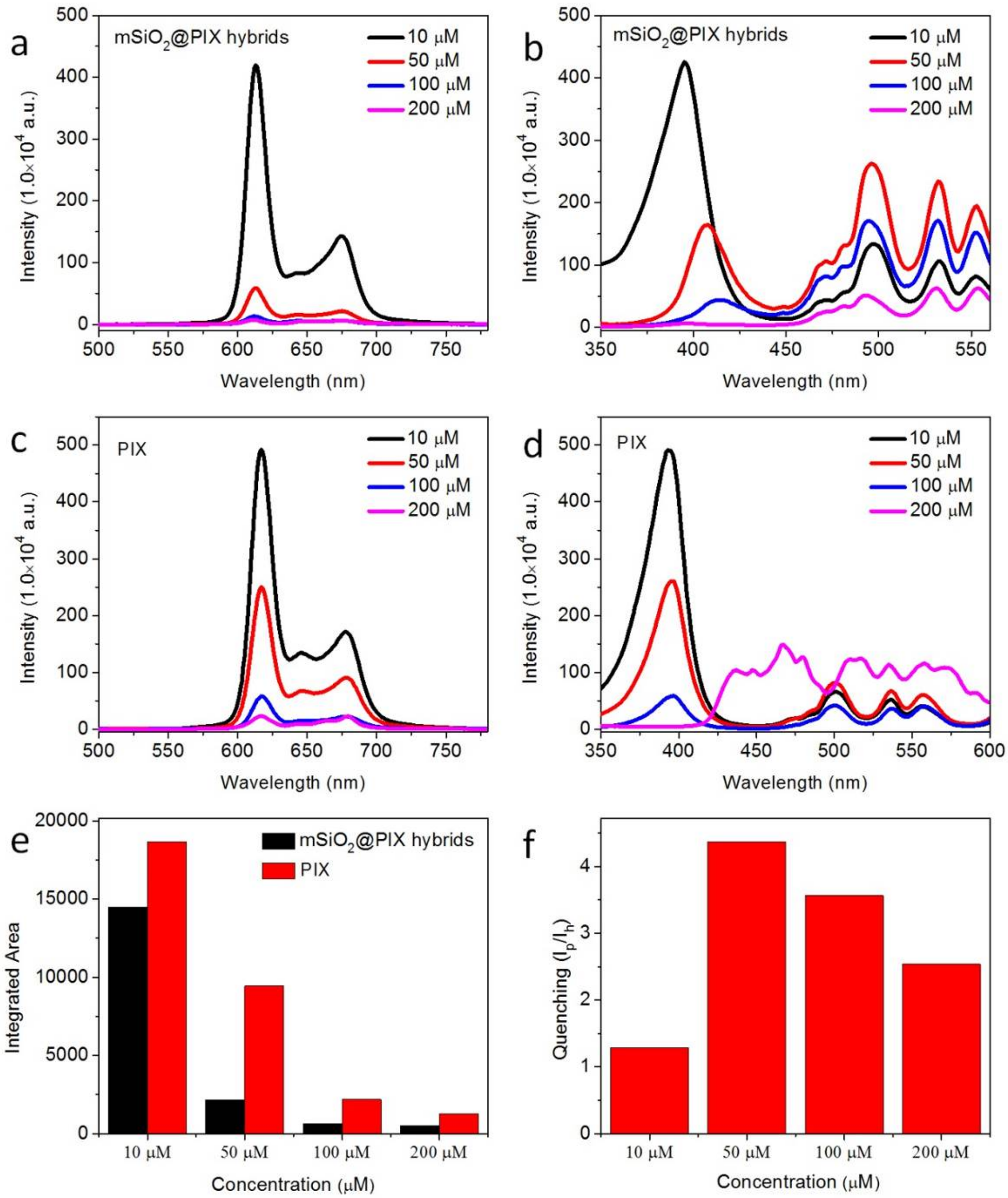

Fig. S10 Photoluminescence spectra of Ag@mSiO_2@PIX hybrid after NaCN treatment and pure PIX of different photosensitizer concentrations. Emission spectra (a) and (c) are excited at 393 nm. Excitation spectra (b) and (d) are emitted at 617 nm. (e) Relationship between integrated fluorescence signal (500-780 nm) and PIX concentration. (f) Relationship between fluorescence quenching of photosensitizer in hybrid (I_p/I_h) and PIX concentration.

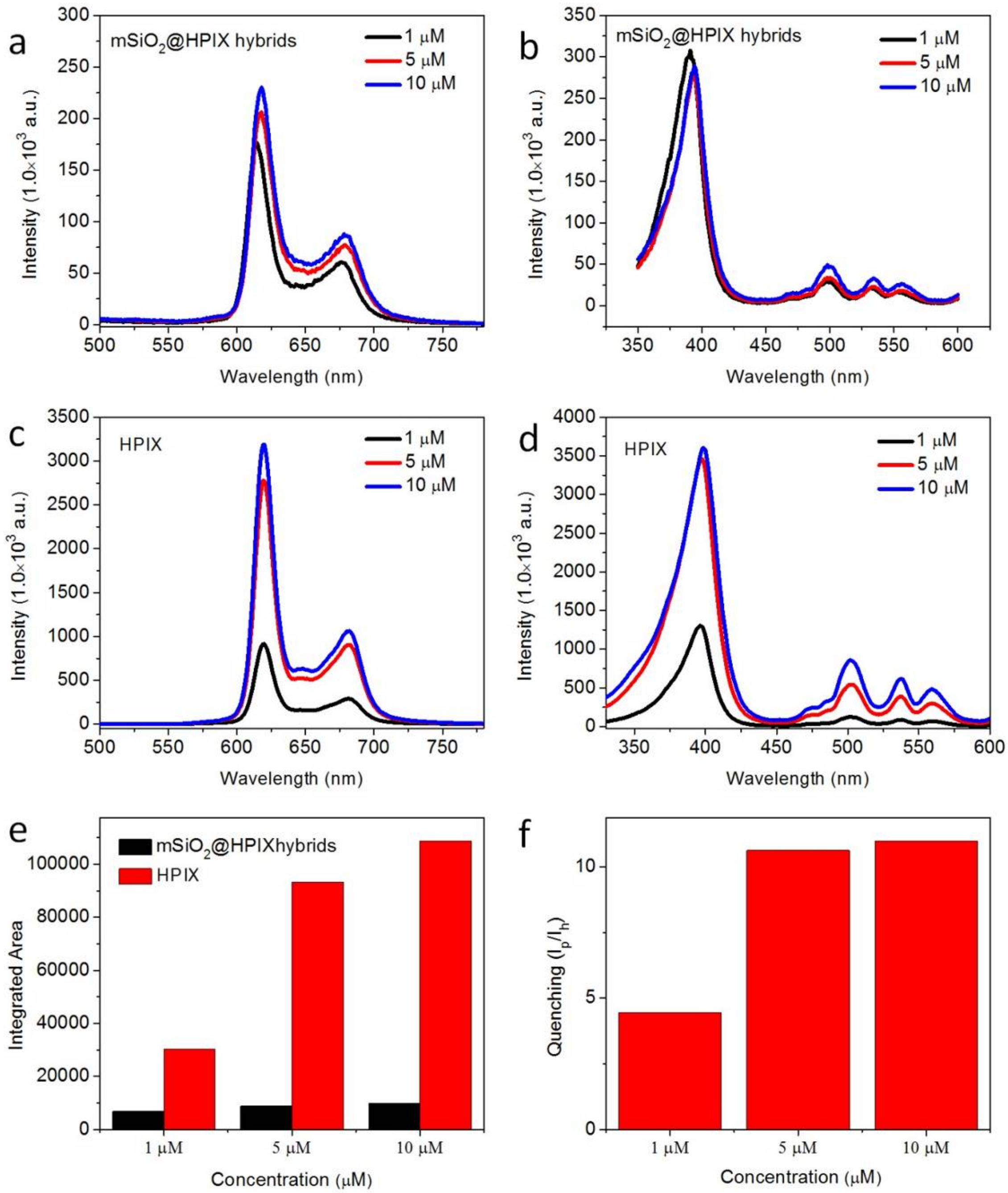

Fig. S11 Photoluminescence spectra of Ag@mSiO$_2$@HPIX hybrid after NaCN treatment and pure HPIX of different photosensitizer concentrations. Emission spectra (a) and (c) are excited at 400 nm. Excitation spectra (b) and (d) are emitted at 614 nm. (e) Relationship between integrated fluorescence signal (500-780 nm) and HPIX concentration. (f) Relationship between fluorescence quenching of photosensitizer in hybrid (I_p/I_h) and HPIX concentration.

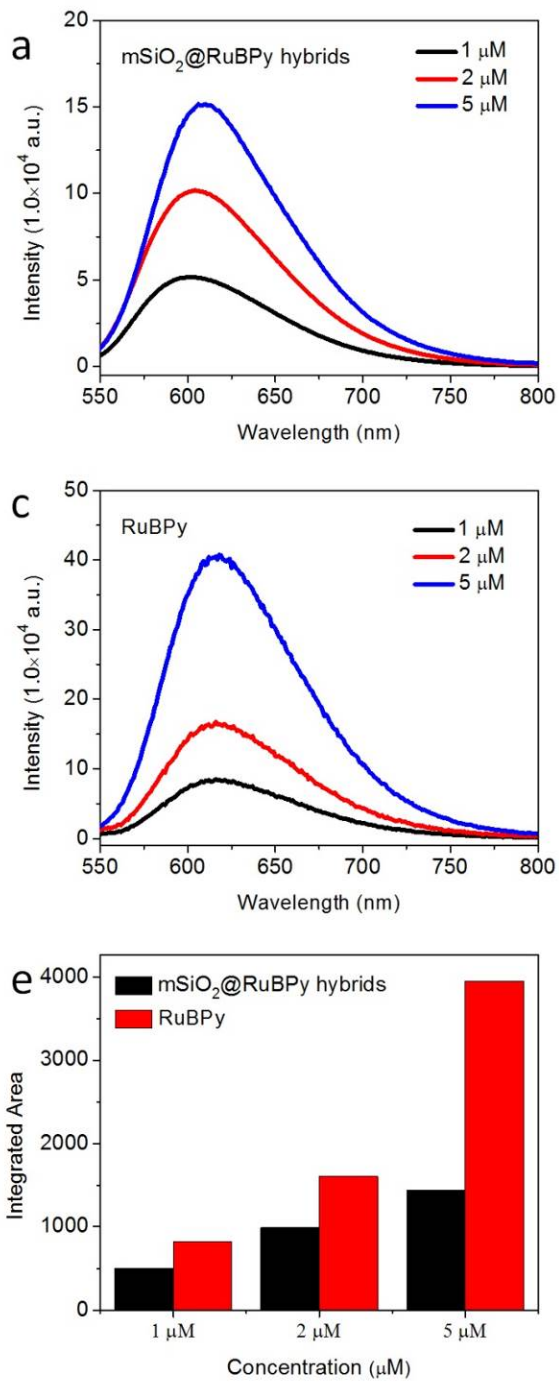

Fig. S12 Photoluminescence spectra of Ag@mSiO$_2$@RuBPy hybrid after NaCN treatment and pure RuBPy of different photosensitizer concentrations. Emission spectra (a) and (c) are excited at 460 nm. Excitation spectra (b) and (d) are emitted at 615 nm. (e) Relationship between integrated fluorescence signal (550-780 nm) and RuBPy concentration. (f) Relationship between fluorescence quenching of photosensitizer in hybrid (I_p/I_h) and RuBPy concentration.

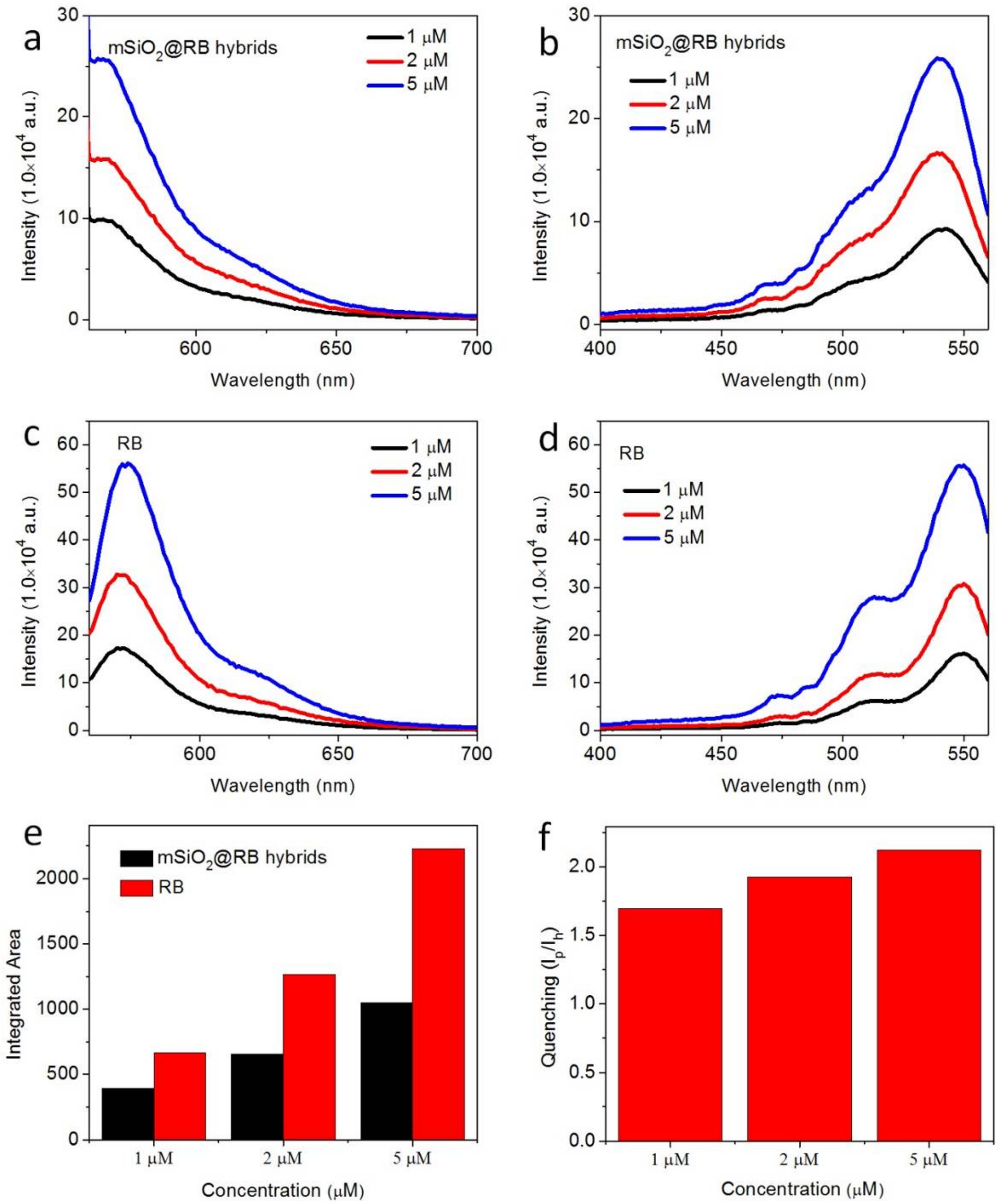

Fig. S13 Photoluminescence spectra of Ag@mSiO$_2$@RB hybrid after NaCN treatment and pure RB of different photosensitizer concentrations. Emission spectra (a) and (c) are excited at 550 nm. Excitation spectra (b) and (d) are emitted at 576 nm. (e) Relationship between integrated fluorescence signal (560-700 nm) and RB concentration. (f) Relationship between fluorescence quenching of photosensitizer in hybrid (I_p/I_h) and RB concentration.

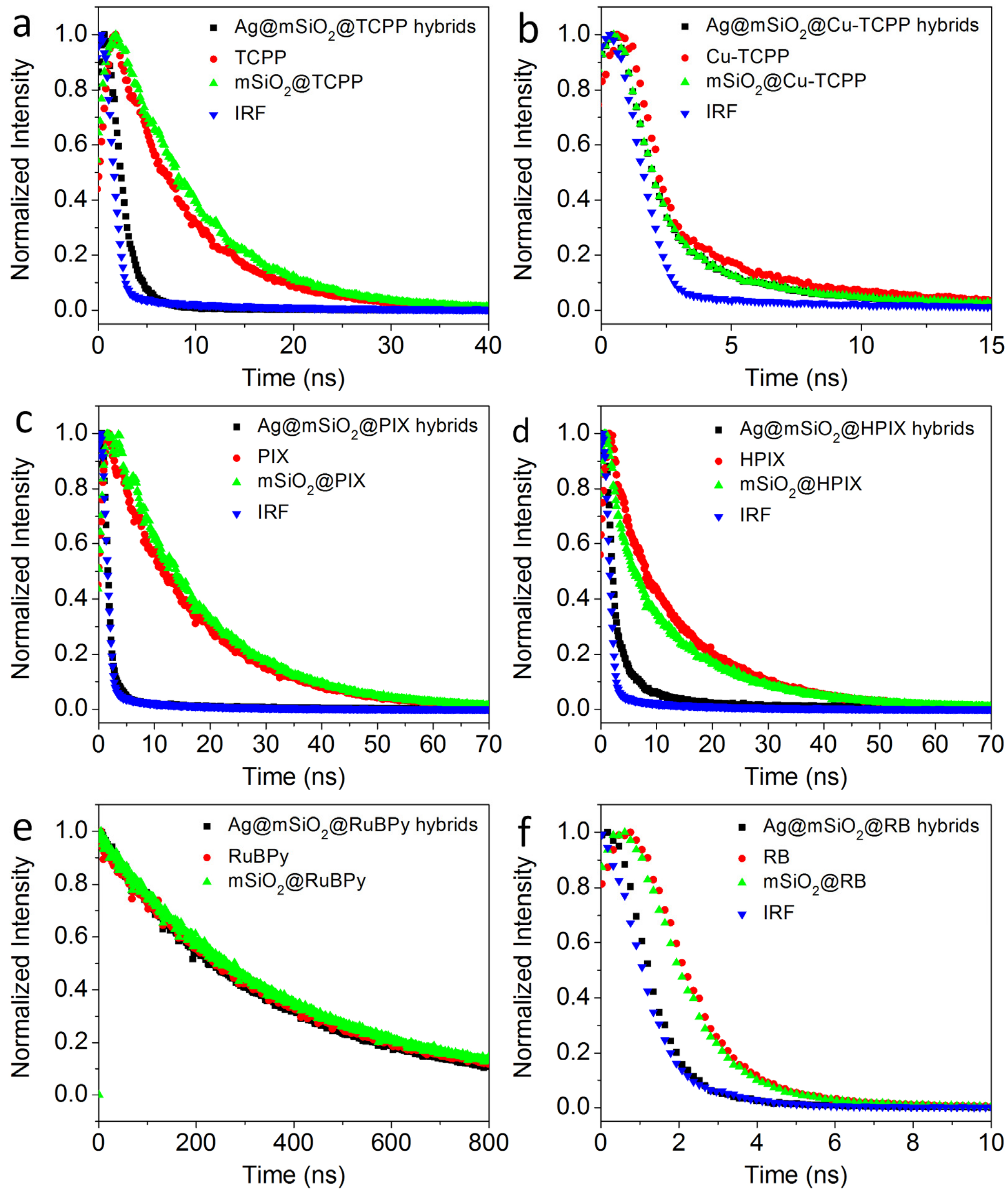

Fig. S14 Time-resolved photoluminescence transient spectra of Ag@mSiO_2@photosensitizers, mSiO_2@photosensitizers and pure photosensitizers, including TCPP (**a**), Cu-TCPP (**b**), PIX (**c**), HPIX (**d**), RuBPy (**e**), and RB (**f**). All photosensitizer concentrations are 10 μM.

Table S1. Results of fluorescence lifetime measurement, where τ_n is amplitude-weighted lifetime and α_n is amplitude.

Samples	τ_1 (ns)	α_1 (%)	τ_2 (ns)	α_2 (%)
Ag@mSiO_2@TCPP hybrid	2.1	100	---	---
TCPP	6.0	100	---	---
mSiO_2@TCPP hybrid	6.1	100	---	---
Ag@mSiO_2@Cu-TCPP hybrid	2.0	100	---	---
Cu-TCPP	2.5	100	---	---
mSiO_2@Cu-TCPP hybrid	2.4	100	---	---
Ag@mSiO_2@PIX hybrid	0.6	100	---	---
PIX	12.8	100	---	---
mSiO_2@PIX hybrid	13.0	100	---	---
Ag@mSiO_2@HPIX hybrid	3.4	4.2	0.2	95.8
HPIX	7.9	100	---	---
mSiO_2@HPIX hybrid	7.6	100	---	---
Ag@mSiO_2@RuBPy hybrid	365.2	93.8	103.2	6.22
RuBPy	365.6	100	---	---
mSiO_2@RuBPy hybrid	364.6	100	---	---
Ag@mSiO_2@RB hybrid	0.2	100	---	---
RB	1.7	100	---	---
mSiO_2@RB hybrid	1.7	100	---	---

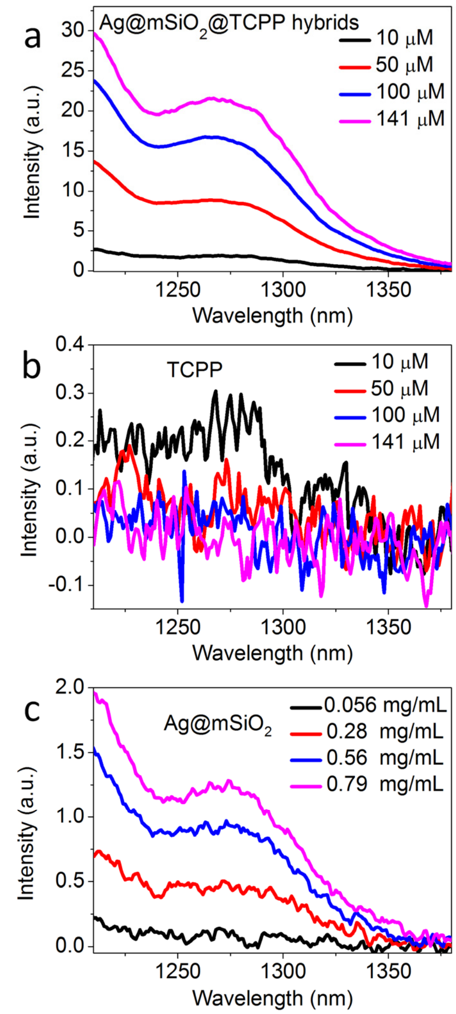

Fig. S15 Singlet oxygen luminescence spectra of Ag@mSiO_2@TCPP hybrids (a), TCPP (b), and the corresponding Ag@mSiO_2 nanoparticles (c).

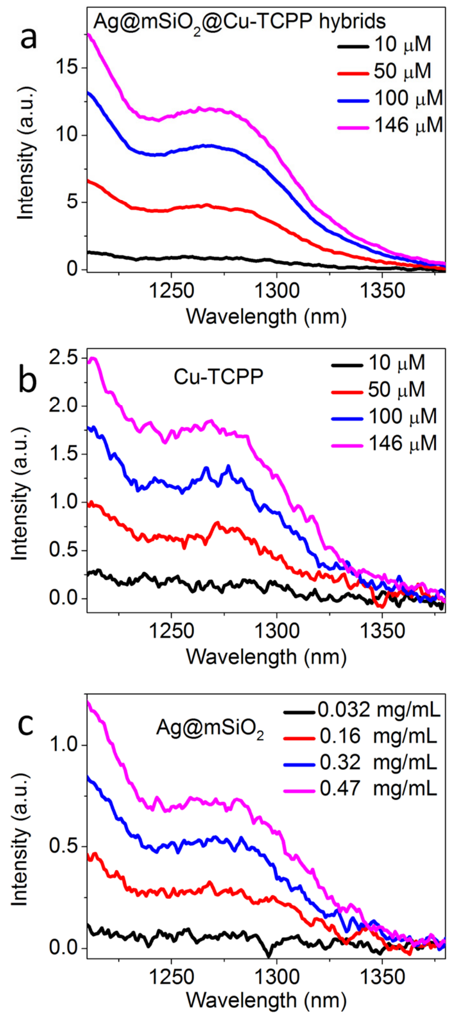

Fig. S16 Singlet oxygen luminescence spectra of Ag@mSiO_2@Cu-TCPP hybrids (a), Cu-TCPP (b), and the corresponding Ag@mSiO_2 nanoparticles (c).

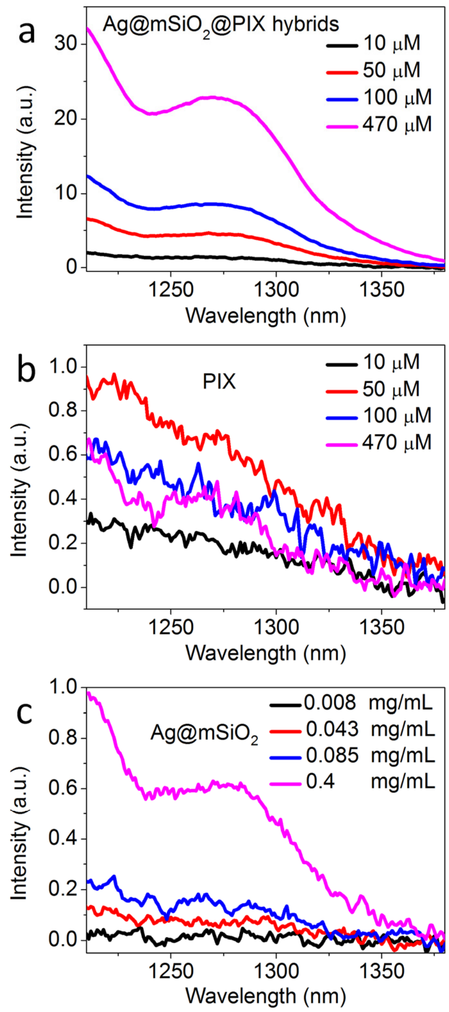

Fig. S17 Singlet oxygen luminescence spectra of Ag@mSiO$_2$@PIX hybrids (a), PIX (b), and the corresponding Ag@mSiO$_2$ nanoparticles (c).

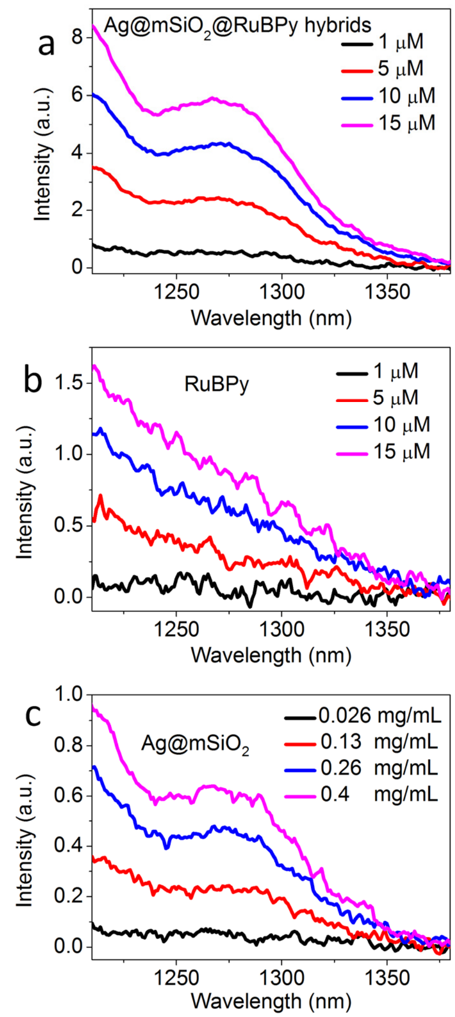

Fig. S18 Singlet oxygen luminescence spectra of Ag@mSiO$_2$@RuBPy hybrids (a), RuBPy (b), and the corresponding Ag@mSiO$_2$ nanoparticles (c).

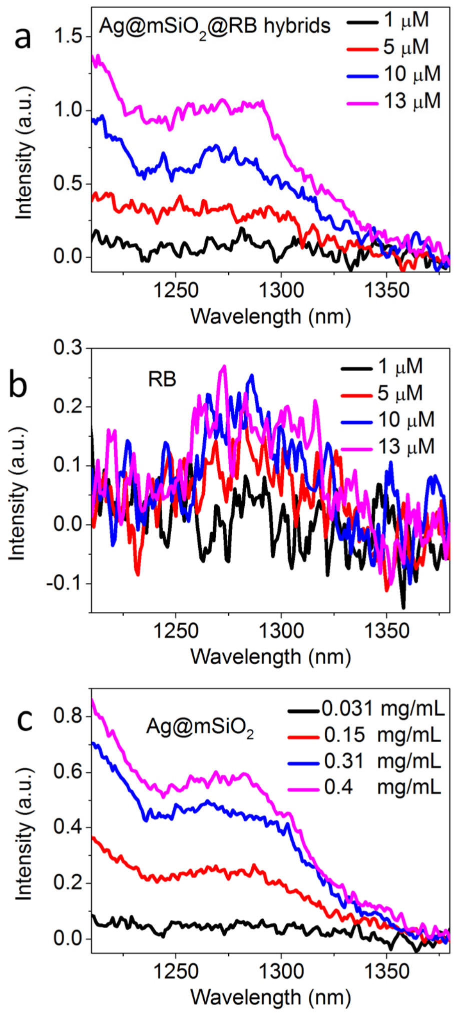

Fig. S19 Singlet oxygen luminescence spectra of Ag@mSiO_2@RB hybrids (a), RB (b), and the corresponding Ag@mSiO_2 nanoparticles (c).

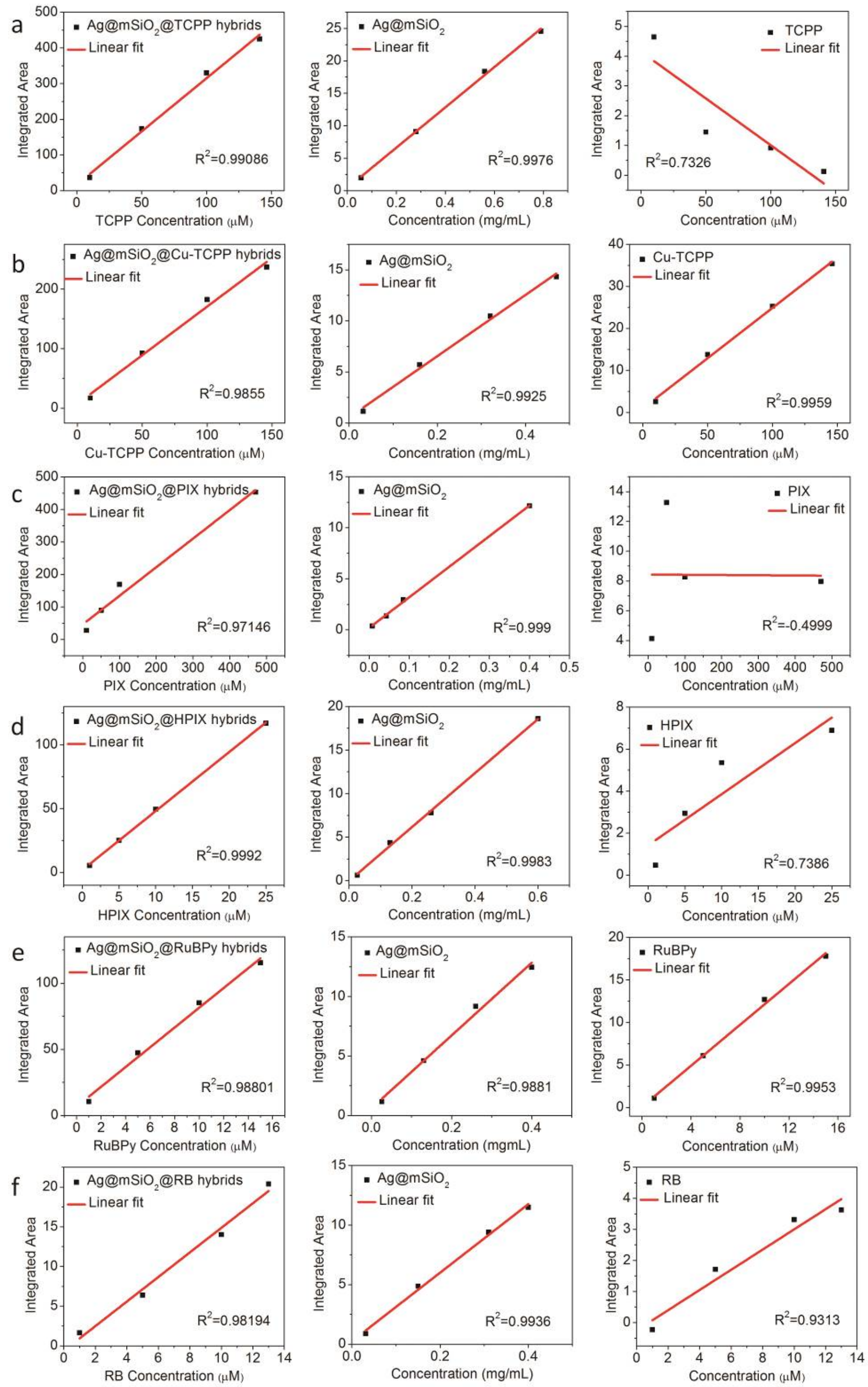

Fig. S20 Relationship between integrated singlet oxygen luminescence signals (1260-1280 nm) and the concentration for Ag@mSiO$_2$@photosensitizer hybrids, Ag@mSiO$_2$ nanoparticles, and photosensitizers, including TCPP (a), Cu-TCPP (b), PIX (c), HPIX (d), RuBPy (e), and RB (f).

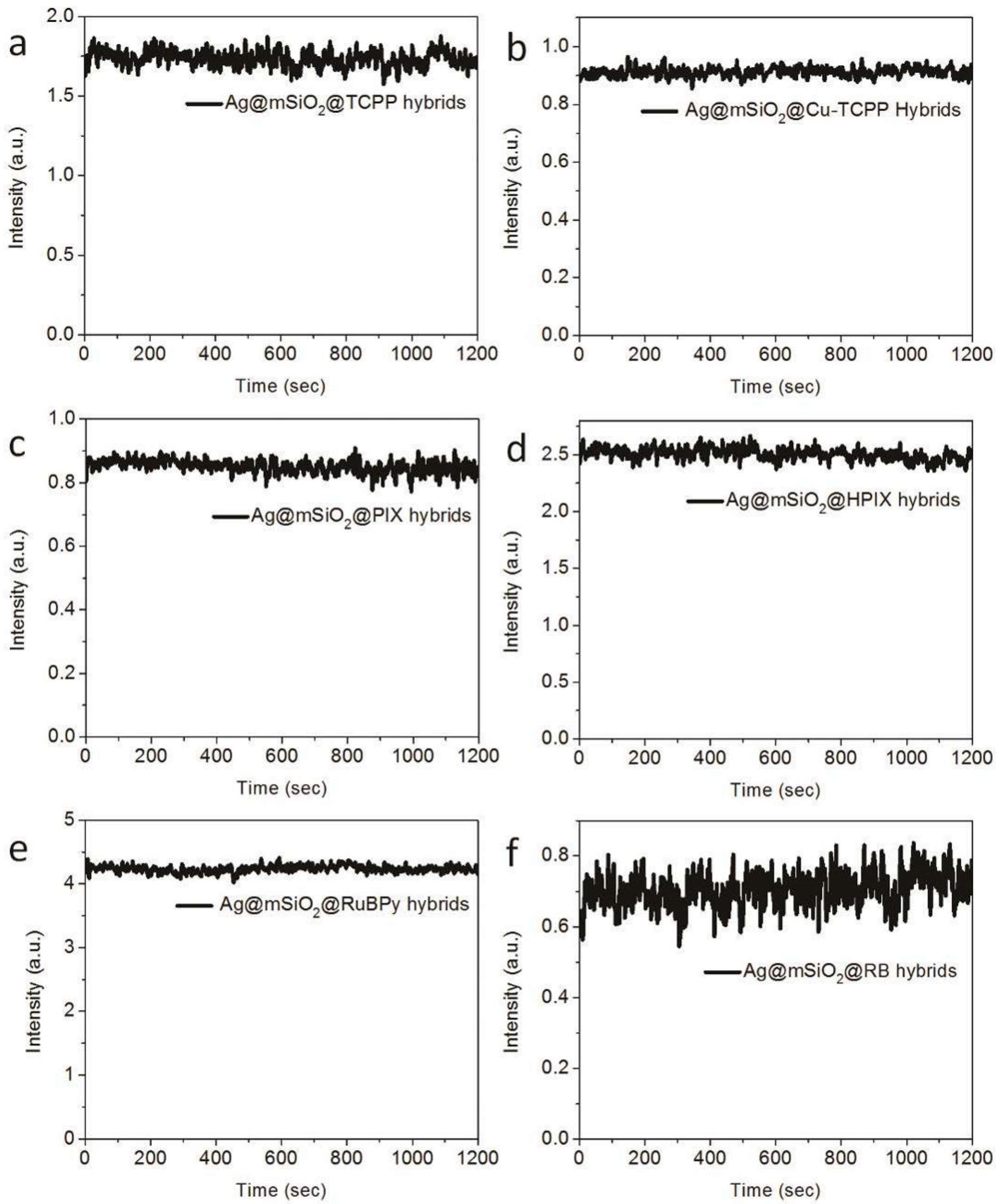

Fig. S21 Photostability of luminescence signal of singlet oxygen produced by the $Ag@mSiO_2@$photosensitizer hybrids with photosensitizer concentration of 10 μM, including, $Ag@mSiO_2@$TCPP (a), $Ag@mSiO_2@$Cu-TCPP (b), $Ag@mSiO_2@$PIX (c), $Ag@mSiO_2@$HPIX (d), $Ag@mSiO_2@$RuBPy (e), and $Ag@mSiO_2@$RB (f).

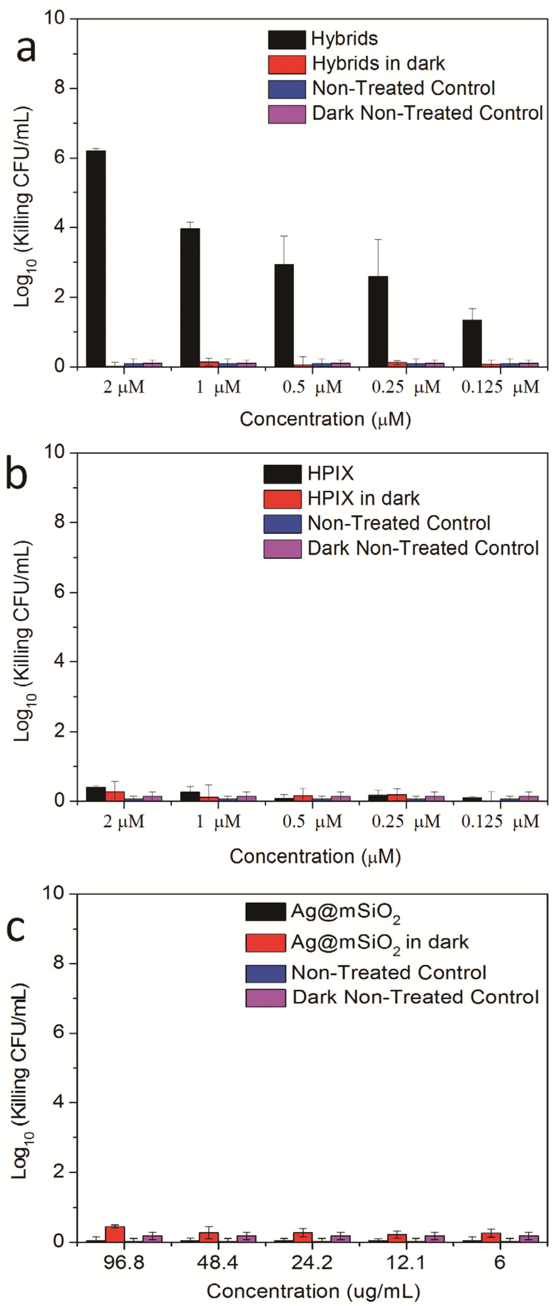

Fig. S22 Antibacterial efficacy of the Ag@mSiO$_2$@HPIX hybrid, pure HPIX and Ag@mSiO$_2$ nanoparticles on *S. epidermidis* (ATCC 35984) with or without light illumination. Killing efficacy is plotted as log$_{10}$ of killing in CFU/mL vs. photosensitizer or Ag@mSiO$_2$ concentration. Bacterial culture was mixed with different concentrations of photosensitizers, followed by light exposure of 40 J/cm^2. Results are expressed as Mean ± SD (n=3).

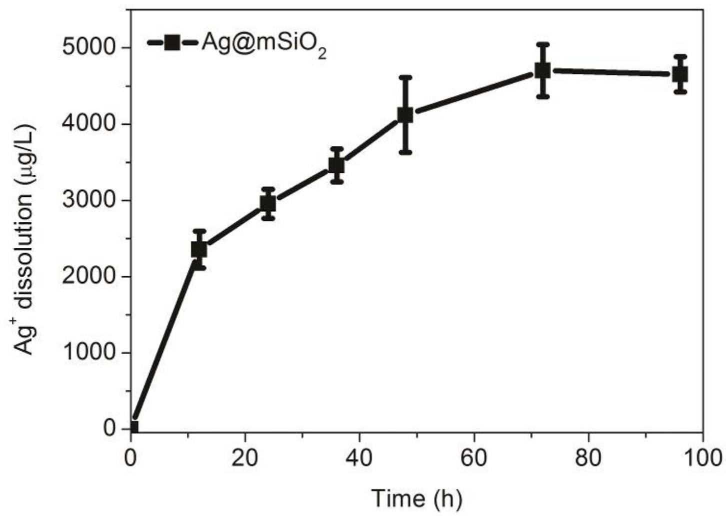

Fig. S23 Ag^{+} release from Ag@mSiO_2 nanoparticles over time under ambient conditions (at pH=4.0).

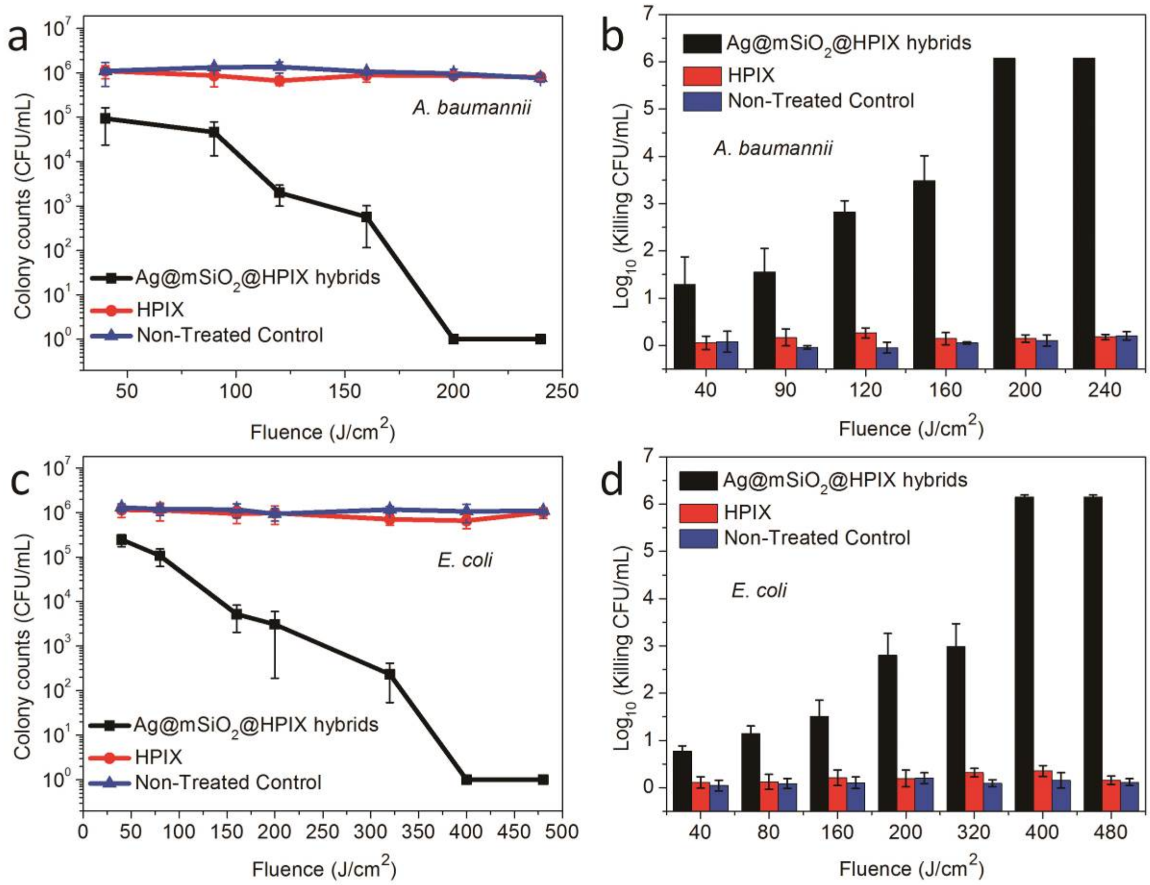

Fig. S24 Antibacterial efficacy of the Ag@mSiO_2@HPIX hybrid and pure HPIX on *A. baumannii* (ATCC 19606) (**a-b**) or *E. coli* (ATCC 35218) (**c-d**). Killing efficacy is plotted as $\log_{10}$ of killing in CFU/mL vs. fluence, where the concentrations of HPIX was fixed at 1 μM. Bacterial culture was mixed with Ag@mSiO_2@HPIX hybrid or HPIX, followed by illumination of 1-5 min (*A. baumannii*), or 1-12 min (*E. coli*). Results are expressed as Mean ± SD (n=3).

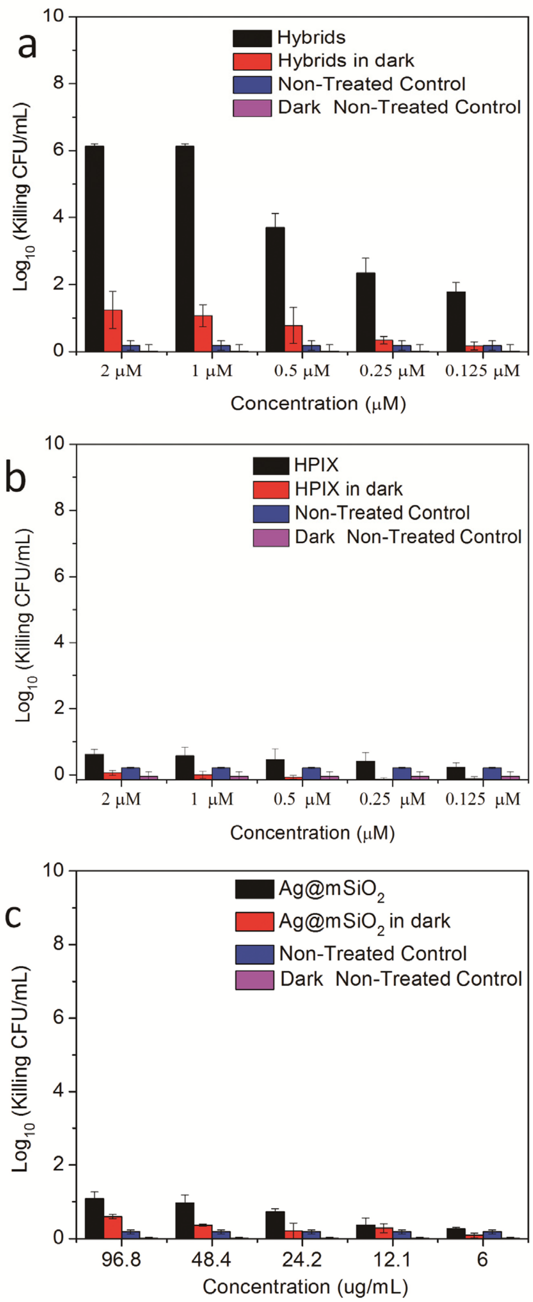

Fig. S25 Antibacterial efficacy of the Ag@mSiO$_2$@HPIX hybrid, pure HPIX and Ag@mSiO$_2$ nanoparticles on *E. coli* (ATCC 35218) with or without light illumination. Killing efficacy is plotted as log$_{10}$ of killing in CFU/mL vs. photosensitizer or Ag@mSiO$_2$ concentration. Bacterial culture was mixed with different concentrations of photosensitizers, followed by light exposure of 400 J/cm^2. Results are expressed as Mean ± SD (n=3).

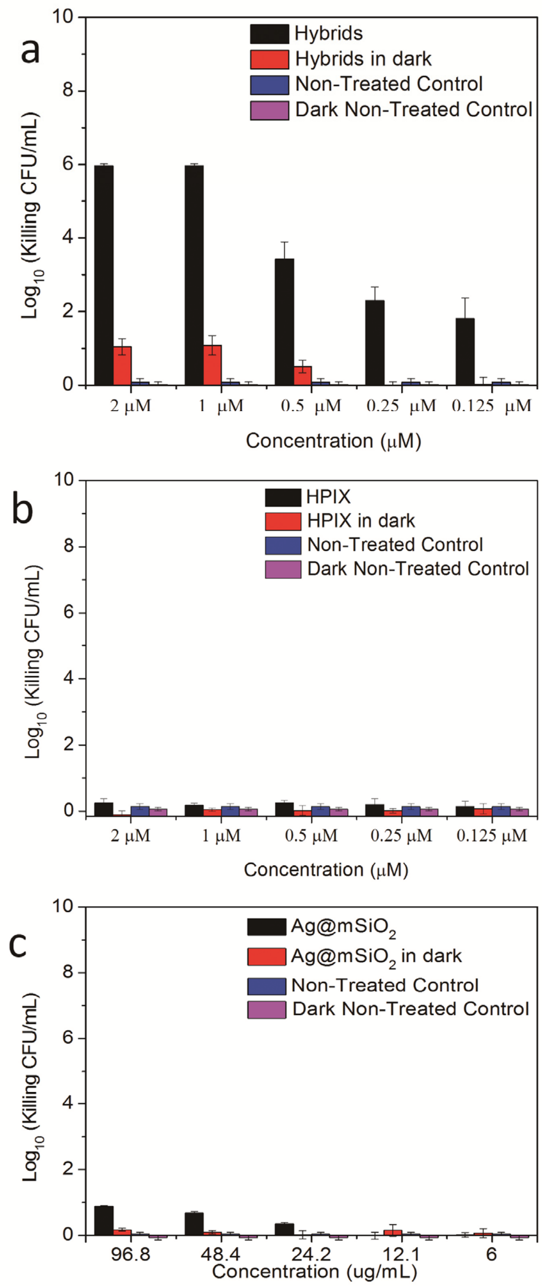

Fig. S26 Antibacterial efficacy of the Ag@mSiO$_2$@HPIX hybrid, pure HPIX and Ag@mSiO$_2$ nanoparticles on *A. baumannii* (ATCC 19606) with or without light illumination. Killing efficacy is plotted as log$_{10}$ of killing in CFU/mL vs. photosensitizer or Ag@mSiO$_2$ concentration. Bacterial culture was mixed with different concentrations of photosensitizers, followed by light exposure of 200 J/cm^2. Results are expressed as Mean ± SD (n=3).

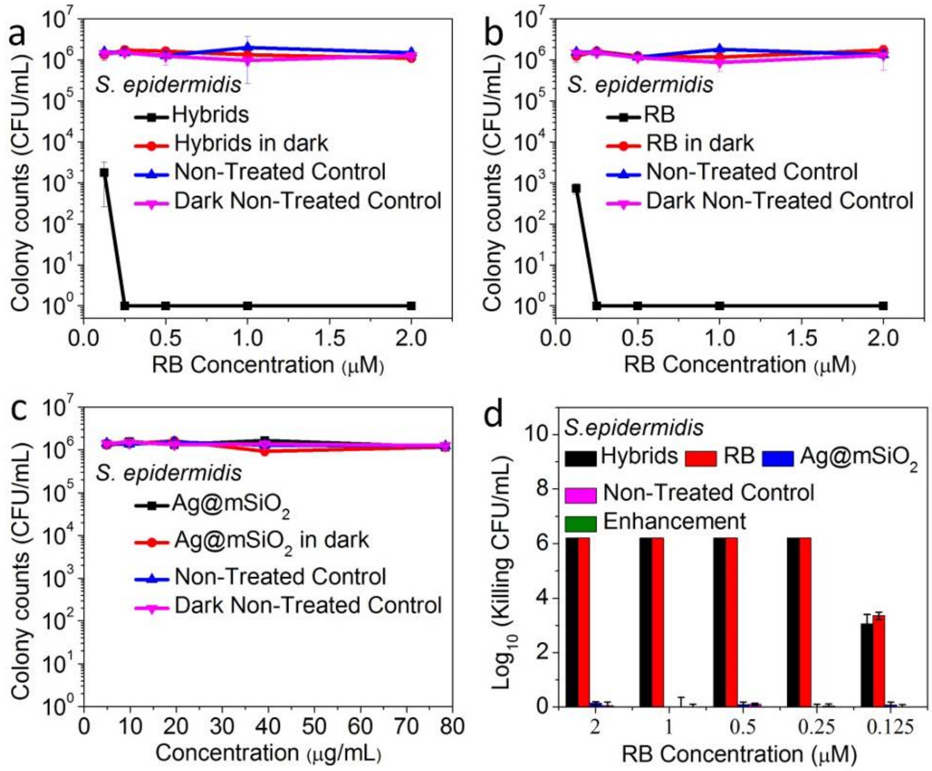

Fig. S27 Antibacterial efficacy of the Ag@mSiO_2@RB hybrid, pure RB and Ag@mSiO_2 nanoparticles on *S. epidermidis* (ATCC 35984) with or without light illumination. Killing efficacy is plotted as $\log_{10}$ of killing in CFU/mL vs. photosensitizer or Ag@mSiO_2 concentration. Bacterial culture was mixed with different concentrations of photosensitizers, followed by light exposure of 40 J/cm^2. Results are expressed as Mean ± SD (n=3).

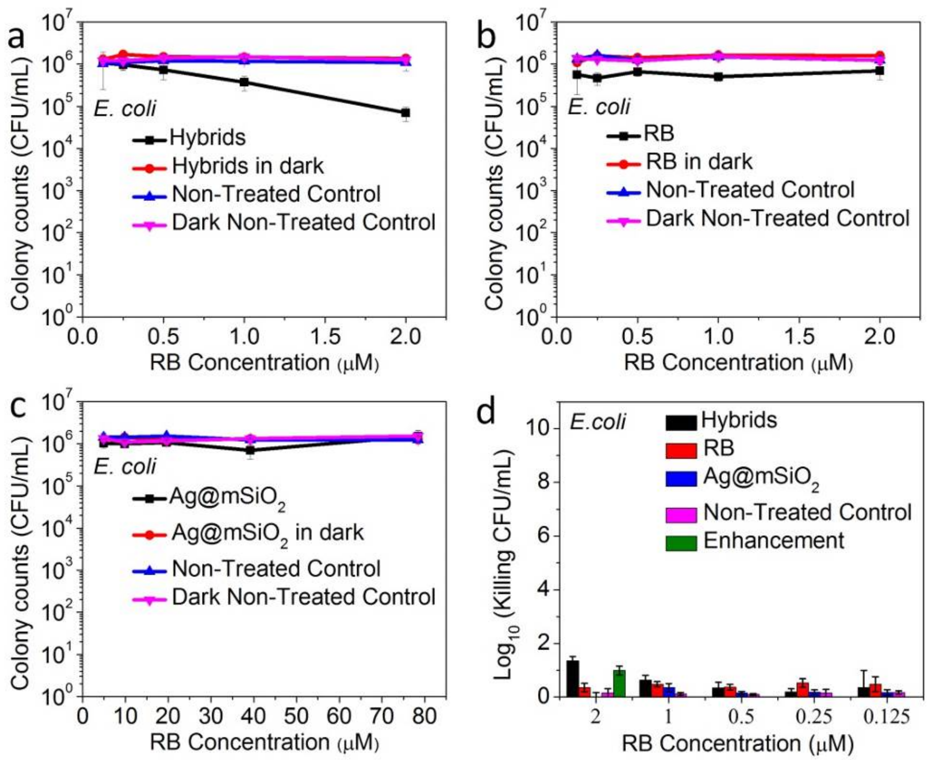

Fig. S28 Antibacterial efficacy of the Ag@mSiO_2@RB hybrid, pure RB and Ag@mSiO_2 nanoparticles on *E. coli* (ATCC 35218) with or without light illumination. Killing efficacy is plotted as $\log_{10}$ of killing in CFU/mL vs. photosensitizer or Ag@mSiO_2 concentration. Bacterial culture was mixed with different concentrations of photosensitizers, followed by light exposure of 400 J/cm^2. Results are expressed as Mean ± SD (n=3).

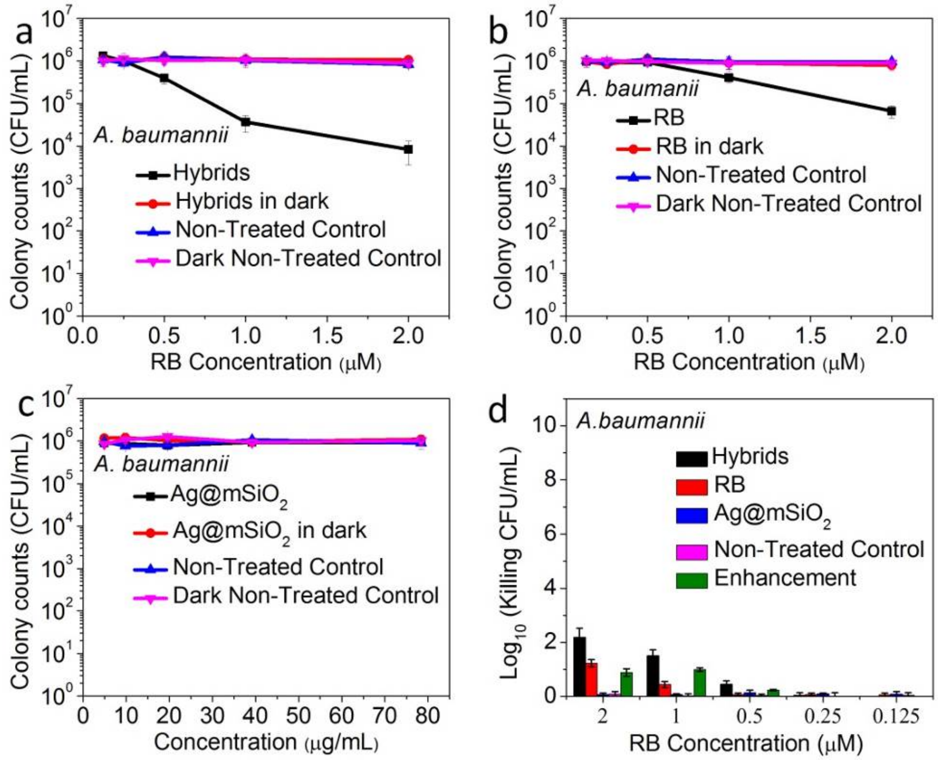

Fig. S29 Antibacterial efficacy of the Ag@mSiO$_2$@RB hybrid, pure RB and Ag@mSiO$_2$ nanoparticles on *A. baumannii* (ATCC 19606) with or without light illumination. Killing efficacy is plotted as log$_{10}$ of killing in CFU/mL vs. photosensitizer or Ag@mSiO$_2$ concentration. Bacterial culture was mixed with different concentrations of photosensitizers, followed by light exposure of 200 J/cm^2. Results are expressed as Mean ± SD (n=3).